Histol Histopathol (2022) 37: 1113-1125

http://www.hh.um.es

Histology and Histopathology
From Cell Biology to Tissue Engineering

ORIGINAL ARTICLE **Open Access**

LncRNA SNHG15 regulates hypoxic-ischemic brain injury via miR-153-3p/SETD7 axis

Jiding Fu[1], Yunbo Huang[2] and Lewu Xian[1]

[1]Department of Intensive Care Unit, Affiliated Cancer Hospital and Institute of Guangzhou Medical University and

[2]Department of Obstetrics, The Third Affiliated Hospital of Guangzhou Medical University, Guangzhou, Guangdong, China

Summary. Hypoxic-ischemic encephalopathy (HIE) is a leading cause of fatality and morbidity in newborns. Long non-coding RNAs (lncRNAs) Small Nucleolar RNA Host Gene 15 (SNHG15) was elevated in the peripheral blood of patients with acute cerebral ischemia, but its role in HI brain injury remained elusive. Hence, this study aimed to investigate the effect of SNHG15 on HI brain injury and study the precise mechanism of action. In this study, a mouse model of HI brain injury was established through ligating right carotid arteries. The oxygen-glucose deprivation (OGD) model was established in PC12 cells. Results showed that SNHG15 was elevated in brain tissues of mice with HI brain injury, and knockdown of SNHG15 attenuated HI-induced impairment of neurobehavioral function, brain edema, brain injury, and cell apoptosis. Besides, SNHG15 acted as a miR-153-3p sponge. SETD7 was identified to be a target of miR-153-3p. Furthermore, down-regulation of SNHG15 inhibited the OGD-induced increase in SETD7 expression in PC12 cells. Moreover, SNHG15 modulated OGD-induced cell apoptosis and decrease of cell viability through the miR-153-3p/SETD7 axis. In conclusion, knockdown of SNHG15 alleviated HI brain injury through modulating the miR-153-3p/ SETD7 axis. SNHG15 may be a prospective target for HIE therapy.

Key words: SNHG15, miR-153-3p, SETD7, Cell apoptosis, Hypoxic-ischemic encephalopathy, Hypoxic-ischemic brain injury

Introduction

Perinatal hypoxic-ischemic encephalopathy (HIE) is a leading cause of fatality and morbidity in newborns (Sun et al., 2014). It is estimated that HIE affects approximately 8 cases per 1000 newborns (Ma et al., 2017). HIE is caused by perinatal asphyxia cerebral ischemia and reperfusion (I/R) (Cao et al., 2020), and results in severe brain injury such as cerebral palsy, learning and memory dysfunction (Lu et al., 2015). Only about 60% of cases with HIE survive, and survivors usually suffer from cognitive impairment and long-term neurological disabilities (Zhao et al., 2020a). At present, many challenges still exist in HIE therapy and effective therapeutic strategies are lacking. Hence, it is urgent to explore promising therapy strategies for patients with HIE.

Long non-coding RNA (lncRNA) Small Nucleolar RNA Host Gene 15 (SNHG15) is an intergenic lncRNA located on chromosome 7p13 (Shen et al., 2017). Recent studies proved that SNHG15 was a cancer regulator, and dysregulation of SNHG15 regulated cancer progression and correlated with prognosis of cancer patients (Kong and Qiu, 2018; Wu et al., 2018; Huang et al., 2019; Mi et al., 2020). For example, highly expressed SNHG15 in papillary thyroid carcinoma promoted cell proliferation, migration and invasion, and inhibited cell apoptosis (Wu et al., 2018). Elevated SNHG15 in breast cancer enhanced cisplatin resistance of cancer cells (Mi et al., 2020). High expression of SNHG15 was associated with lymphnode metastasis, liver metastasis and poor prognosis of colorectal cancer patients (Huang et al., 2019). At present, there are many studies focused on

Corresponding Author: Lewu Xian, Department of Intensive Care Unit, Affiliated Cancer Hospital and Institute of Guangzhou Medical University, 78 hengzhigang Road, Yuexiu District, Guangzhou, Guangdong, 510000, China. e-mail: lewuxianlwx@163.com

DOI: 10.14670/HH-18-489

Abbreviations. HIE, Hypoxic-ischemic encephalopathy; lncRNAs, long non-coding RNAs; SNHG15, Small nucleolar RNA host gene 15; OGD, Oxygen glucose deprivation; SETD7, SET Domain Containing 7; CCK-8, Cell counting kit-8; I/R, ischemia and reperfusion; CDC6, cell division cycle 6; MIAT, Myocardial infarction associated transcript; CeRNA: competing endogenous RNA; PTCSC3, Papillary Thyroid Carcinoma Susceptibility Candidate 3; NBR2, neighbour of BRCA1 gene 2; SNHG3: small nucleolar RNA host gene 3.

exploring the role of SNHG15 in cancers, but its role in HI brain injury remains elusive.

LncRNAs belong to the non-coding RNAs (ncRNA) family with over 200 nt in length and no protein-coding capacity (Li et al., 2020). LncRNAs exhibit aberrant expression in many diseases and participate in disease regulation. For example, overexpressed lncRNA cell division cycle 6 (CDC6) promoted breast cancer progression through regulating cancer cell proliferation and migration (Kong et al., 2019). Highly expressed lncRNA THRIL in the lung of mice with sepsis aggravated sepsis-induced acute lung injury (Chen et al., 2020). Furthermore, studies revealed that some lncRNAs also played essential roles in HI brain injury (Li et al., 2019; Zhao et al., 2020a). For example, elevated lncRNA myocardial infarction associated transcript (MIAT) attenuated neuron apoptosis in a neonatal rat model of HI injury via regulating miR-211/GDNF axis (Li et al., 2019). LncRNA NEAT1 was elevated in neonatal mice with HI brain injury, and overexpressed lncRNA NEAT1 alleviated HI brain injury (Zhao et al., 2020a). Therefore, lncRNAs may exert vital roles in the development of HI brain injury.

Recent studies described that lncRNAs modulated gene expression via a post-transcriptional mechanism, thereby playing vital roles in multiple disease regulation (Geisler and Coller, 2013). Specifically, the competing endogenous RNA (ceRNA) hypothesis proposed that lncRNAs might act as microRNA (miRNA) sponges, thereby alleviating inhibition effects of miRNAs on target mRNAs at a post-transcriptional level (Abdollahzadeh et al., 2019; Cong et al., 2019). For example, lncRNA Papillary Thyroid Carcinoma Susceptibility Candidate 3 (PTCSC3) inhibited the cervical cancer cell proliferation, invasion, and migration ability through sponging miR-574-5p (Tong et al., 2020). LncRNA neighbour of BRCA1 gene 2 (NBR2) inhibited migration and invasion of colorectal cancer cells by regulating the expression of miR-21 (Bai et al., 2020). Interestingly, some lncRNAs also could regulate HI brain injury via a ceRNA mechanism (Fang et al., 2019; Yang et al., 2020). For example, lncRNA small nucleolar RNA host gene 3 (SNHG3) was decreased in neonatal brain with HI brain damage, and it protected against HI-induced neonatal brain injury though regulating the expression of XIAP and CAAP1 via acting as a miR-196 sponge (Yang et al., 2020). LncRNAs MALAT1 regulated apoptosis of hippocampal neurons in HI brain damage by modulating the expression of WNT1 via sponging miR-429 (Fang et al., 2019). As a member of lncRNAs, SNHG15 was elevated in acute ischemic stroke patients (Deng et al., 2018). Wen et al. showed that inhibition of SNHG15 alleviated cerebral ischemia-reperfusion injury through miR-183-5p/FOXO1 axis (Wen et al., 2020). Therefore, we inferred that SNHG15 might participate in the regulation of HI brain injury. Hence, this study aimed to investigate the effect of SNHG15 on HI brain injury and explore the detailed mechanism of action.

Materials and methods

Establishment of mouse model of HI brain injury

Forty eight male C57BL/6 mice aged 7 days were obtained from Beijing Laboratory Animal Research Center (Beijing, China). All mice were allocated into four groups (10 mice in each group), including the sham group, HI group, HI+sh-SNHG15 group, and HI+sh-NC group. The mouse model with HI brain injury was established based on previous studies (Rice et al., 1981; Xue et al., 2019). To establish the HI brain injury model, mice were anesthetized by 2% isoflurane (Cat. # 792632, Sigma, St. Louis, MO, USA). The right carotid artery of mice in the HI group was ligated for 5 min and recovered for 2 h after ligation. Subsequently, the mice were placed into a chamber with 8% oxygen and 92% nitrogen for 2.5 h at 37°C. Different from HI group, the mice in the HI+sh-SNHG15 group and HI+sh-NC group were injected with lentivirus expressing shRNA against SNHG15 or shRNA negative control before HI treatment. The mice in the sham group underwent a sham operation without carotid artery ligation or hypoxic treatment. The schematic of the in vivo experimental procedure is presented in Fig. 1. All protocols were conducted according to the guidelines for the care and use of laboratory animals. The Experimental Animal Ethics of Affiliated Cancer Hospital & Institute of Guangzhou Medical University permitted this study.

Elevated plus-maze

The neurobehavioral function impairment induced by HI brain injury was explored after 4 weeks of brain injury establishment by elevated plus-maze as previously described (Rostami et al., 2012). The elevated plus-maze contained two open arms and two closed arms. The height of the maze above the floor was 50 cm. The arms of the apparatus were manufactured into a ‘‘+’’ shape. Mice were placed in the maze center facing a closed arm. Afterward, all mice were permitted to explore the maze for 5 min without interference. During the test, the behavioral patterns, including the time spent in open arms, head dips time, time spent in closed arms, time rearing, and time spent in novel object, were recorded.

Water content determination

After mice were anesthetized and sacrificed after 24 h of brain injury establishment, water content of brain samples was determined. The wet weight was measured immediately after the ipsilateral hemisphere was obtained. Subsequently, the brain samples were transferred to an 100°C oven for 72 h, and then the dry weight of the ipsilateral hemisphere was weighed (Zhang et al., 2016). The brain water content was calculated based on the formula: ((wet weight − dry weight)/wet weight) × 100%.

TTC staining

TTC staining was performed to evaluate infarction volume after 24 h of brain injury establishment. After mice were anesthetized and sacrificed, the brain was collected and moved to −20°C for 10 min, and then made into coronal sections with 2 mm thickness. Afterward, the sections were immersed into 2% TTC solution for 25 min at 37°C, and fixed in 4% formaldehyde. Finally, infarction volume of brain was analyzed by ImageJ software (Tu et al., 2018).

HE staining

Hippocampus tissues of mice were resected after 24h of brain injury establishment and fixed using paraformaldehyde and embedded in paraffin. Then, the tissues were cut into 5 μm slices. The slices were stained with hematoxylin and eosin. The staining sections were analyzed under a light microscope (Olympus, Japan).

TUNEL staining

Hippocampus tissues of mice were resected after 24 h of brain injury establishment and fixed using paraformaldehyde and embedded in paraffin. Then, the tissues were cut into 5 μm slices. The TUNEL Assay Kit (Cat. # C10618, Thermo Fisher Scientific, Waltham, MA, USA) was employed to conduct TUNEL staining following the manufacturer's protocols. The apoptosis proportion was analyzed based on the number of TUNEL-positive cells and total cells.

Caspase-3 activity determination

Cell apoptosis was evaluated by determining the caspase-3 activity of hippocampus tissues after 24h of brain injury establishment. After the lysates of hippocampus tissues were obtained, the activity of caspase-3 was measured using Caspase 3 Colorimetric Assay Kit (Cat. #CASP3C, Sigma, St. Louis, MO, USA) following the manufacturer's protocols. The relative caspase-3 activity was calculated by recording optical density values at 405 nm and normalizing to the sham group.

Establishment of oxygen-glucose deprivation (OGD) model

PC12 cells were purchased from Shanghai Institute of Cell Biology, Chinese Academy of Sciences (Shanghai, China). The cells were maintained in DMEM medium supplemented with 10% heat-inactivated horse serum, 5% fetal bovine serum and 100 U/ml penicillin, and 100 μg/ml streptomycin at 37°C with 5% CO_2 and 95% air. To establish the OGD model, PC12 cells were cultured in glucose-free DMEM at 37°C in an oxygen-free chamber (5% CO_2 and 95% N_2) for 4h, then maintained in normal condition for 24 h (Zhu et al., 2010). PC12 cells maintained in normal glucose and normoxic atmosphere were used as the control.

Quantitative real-time polymerase chain reaction (qRT-PCR)

Total RNA was extracted using TRIzol reagent, and cDNA was generated utilizing the cDNA Synthesis Kit (Cat. # 11117831001, Sigma, St. Louis, MO, USA). SYBR Green Master Mix (Cat. # A46109, Thermo Fisher Scientific, Waltham, MA, USA) was employed to perform qPCR assay. The PCR conditions were: 95˚C for 5 min; 40 cycles of 95˚C for 10 sec, 60˚C for 30 sec and 72˚C for 10 sec; 72°C for 10 min. The primers of lncRNA SNHG15, miR-153-3p, and SETD7 are presented below:
lncRNA SNHG115: F, 5'-GCTGAGGTGACGG TCTCAAA-3', R: 5'-GCCTCCCAGTTTCATGGACA-3' (Ye et al., 2019); miR-153-3p: F, 5'- ACACTCCA GCTGGGTTGCATAGTCACAAA-3', R: 5'-CAGT GCGTGTCGTGGAGT-3' (Sun et al., 2018); SETD7: F, 5'- CCTGGTGGAAGTTAGGTGCTA-3', R, 5'-CGG TGTCTCTAATGCCTCTGA-3' (Zhao et al., 2020b). The relative expressions of lncRNA SNHG15, miR-153-3p, and SETD7 were analyzed using the $2^{-\Delta\Delta Ct}$ method through normalizing to *GAPDH* or U6.

Cell transfection

The siRNAs against lncRNA SNHG15 and SETD7 were generated from GenePharma (GenePharma, Shanghai, China). miR-153-3p mimics and inhibitor were purchased from Ribobio (Ribobio, Guangzhou, China). The siRNAs, mimics, and inhibitor were transfected into PC12 cells by Lipofectamine 3000 (Cat. # L3000015, Thermo Scientific, Waltham, MA, USA) under the manufacturer's instructions. The transfection efficiency was determined using qRT-PCR.

Luciferase assay

The putative sequences of lncRNA SNHG15 binding to miR-153-3p (wild and mutant types), and 3'-UTR of SETD7 (wild and mutant types) were cloned into the psiCHECK-2 vector (Cat. #C8021, Promega, Madison, WI, USA). The mutant sequences of lncRNA SNHG15 and mutant 3'-UTR of SETD7 were generated from GenePharma (GenePharma, Shanghai, China). The fused psiCHECK-2 vector and miR-153-3p mimics were transfected into PC12 cells. After 48h, the PC12 cells were harvested to measure the relative luciferase activity using the Dual-luciferase reporter assay system (Cat. #E1910, Promega, Madison, WI, USA).

Western blot

The lysates of tissues and PC12 cells were extracted using RIPA buffer (Cat. #E1910, Thermo Fisher Scientific, Waltham, MA, USA) and quantified by a

BCA kit (Cat. #71285-M, Sigma, St. Louis, MO, USA). Then, the lysates were separated by SDS-PAGE and transferred to PVDF membranes. After blocking in 4% non-fat milk, the membranes were probed with anti-SETD7 (Cat. #ab189347, 1:1000) and GAPDH (Cat. #ab9485, 1:2500) antibodies (Abcam, Cambridge, MA, UK) overnight at 4°C, followed by incubation with IgG H&L (HRP) (Cat. #ab6721, Abcam, Cambridge, MA, UK) for 2h at 22°C. GAPDH was used as a control protein. The signals of blots were determined though the ECL Plus Western Blotting Substrate (Cat. # 32134, Thermo Fisher Scientific, Waltham, MA, USA).

Cell counting kit-8 (CCK-8) assay

PC12 cells were trypsinized and inoculated into 96-well plates (2000 cells/well). Then, cells were maintained in 37°C cell incubator with 5% CO_2. Seventy-two hours later, cells were incubated with 10 μL of CCK-8 reagent (Cat. # 96992, Sigma, St. Louis, MO, USA) for 1h at 37°C. Cell viability was calculated by measuring the values of optical density at 450 nm.

Determination of lactate dehydrogenase (LDH) level

To assess cell injury, LDH level in transfected PC12 cells was determined. After cell culture supernatant was collected, the LDH level was measured using LDH Commercial assay kits (Cat. #ab102526, Abcam, Cambridge, UK) following the manufacturer's protocols.

Flow cytometry

Cell apoptosis was evaluated using Annexin V-FITC Apoptosis Detection Kit (Cat. #APOAF, Sigma, St. Louis, MO, USA). PC12 cells were trypsinized after 48 h of transfection and washed in PBS. The harvested cells were resuspended using the binding buffer and incubated with Annexin-V and PI in the dark for 15 min. The stained cells were determined using Flow Cytometry (BD, San Jose, CA, USA).

Statistical analysis

Data processing was completed by SPSS Statistics 22.0 (SPSS, Chicago, IL, USA). All data were presented as mean ± standard deviation (SD). The differences among groups were analyzed using one-way ANOVA with LSD's post hoc test. The criteria of the statistically significant difference was $P<0.05$.

Results

Knockdown of SNHG15 attenuated HI-induced impairment of neurobehavioral function and brain edema

To investigate the role of SNHG15 in HI brain injury, the mouse model with HI brain injury was established. QRT-PCR assay proved that SNHG15 was elevated in brain tissues of mice with HI ($P<0.001$, Fig. 2A). Therefore, the shRNA against SNHG15 was

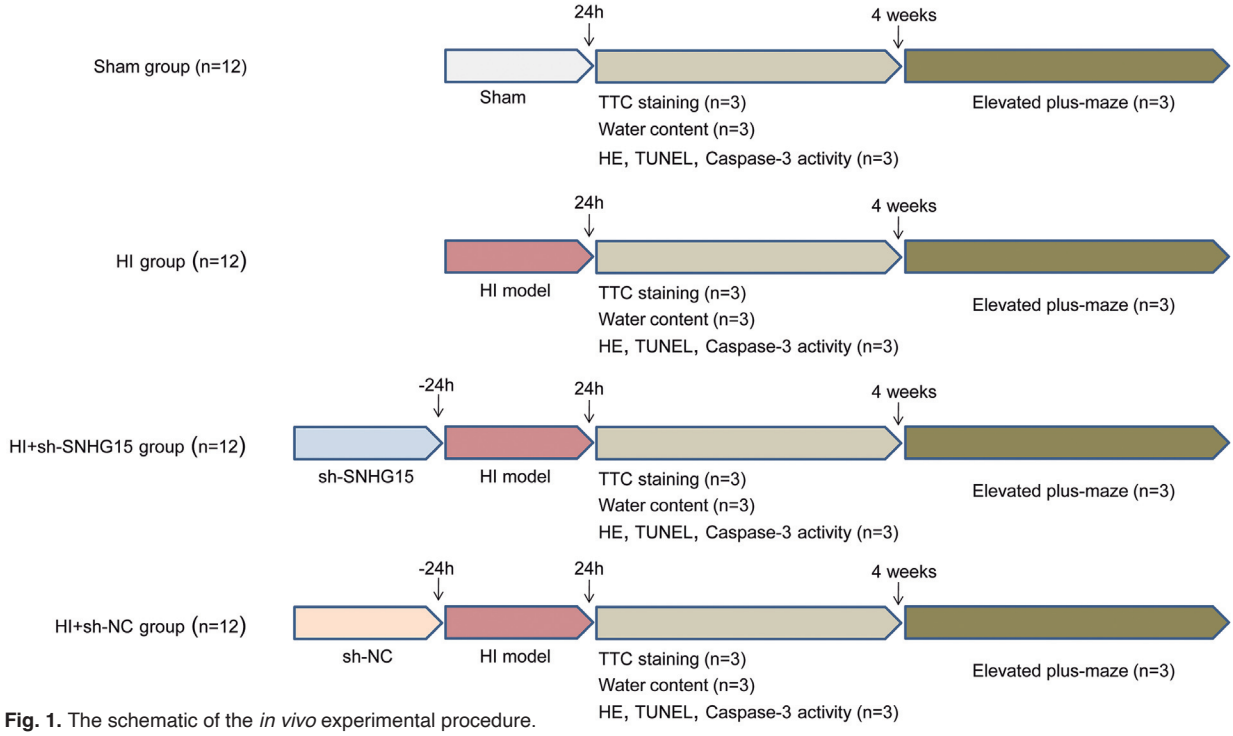

Fig. 1. The schematic of the *in vivo* experimental procedure.

introduced into the HI model to knockdown SNHG15, which was verified by qRT-PCR assay (P<0.001, Fig. 2A). The elevated plus-maze experiment presented that the time spent in open arms and head tips were increased in mice with HI injury, but was reversed by shRNA against SNHG15 (P<0.05, Fig. 2B,C). However, the time spent in closed arms, rearing and novel object were decreased in HI injury mice, which was increased by shRNA against SNHG15 (P<0.05, Fig. 2D-F). Besides, down-regulated SNHG15 inhibited the elevated water content of mice in HI group (P<0.05, Fig. 2G). Therefore, knockdown of SNHG15 attenuated HI-induced neurobehavioral function impairment and brain edema.

Knockdown of SNHG15 attenuated HI-induced brain injury and cell apoptosis

To better understand the effect of SNHG15 on HI brain injury, infarction volume of brain was explored by performing TTC staining. Results exhibited that SNHG15 knockdown suppressed the HI-induced brain infarction (all P<0.001, Fig. 3A). HE staining result revealed that cells in sham groups appeared with regular arrangements and intact nuclei (Fig. 3B). However, disrupted cell arrangements and decreased cell density were presented in cells of the HI group, which were reversed by down-regulation of SNHG15 (Fig. 3B). Besides, HI injury induced inflammation response of hippocampus tissues, but the action was inhibited by down-regulation of SNHG15 (all P<0.001, Fig. 3B,C). Furthermore, HI injury induced cell apoptosis of hippocampus tissues (P<0.001), which was abrogated by down-regulated SNHG15 (P<0.01, Fig. 3D,E). Moreover, caspase-3 activity was increased in the HI group compared to the sham group (P<0.001), but was decreased by decreased SNHG15 (P<0.01, Fig. 3F). Thus, these results indicated that SNHG15 knockdown attenuated HI-induced brain injury and cell apoptosis.

SNHG15 acted as a miR-153-3p sponge

LncRNAs usually modulate gene expression through functioning as the miRNA sponges (Abdollahzadeh et

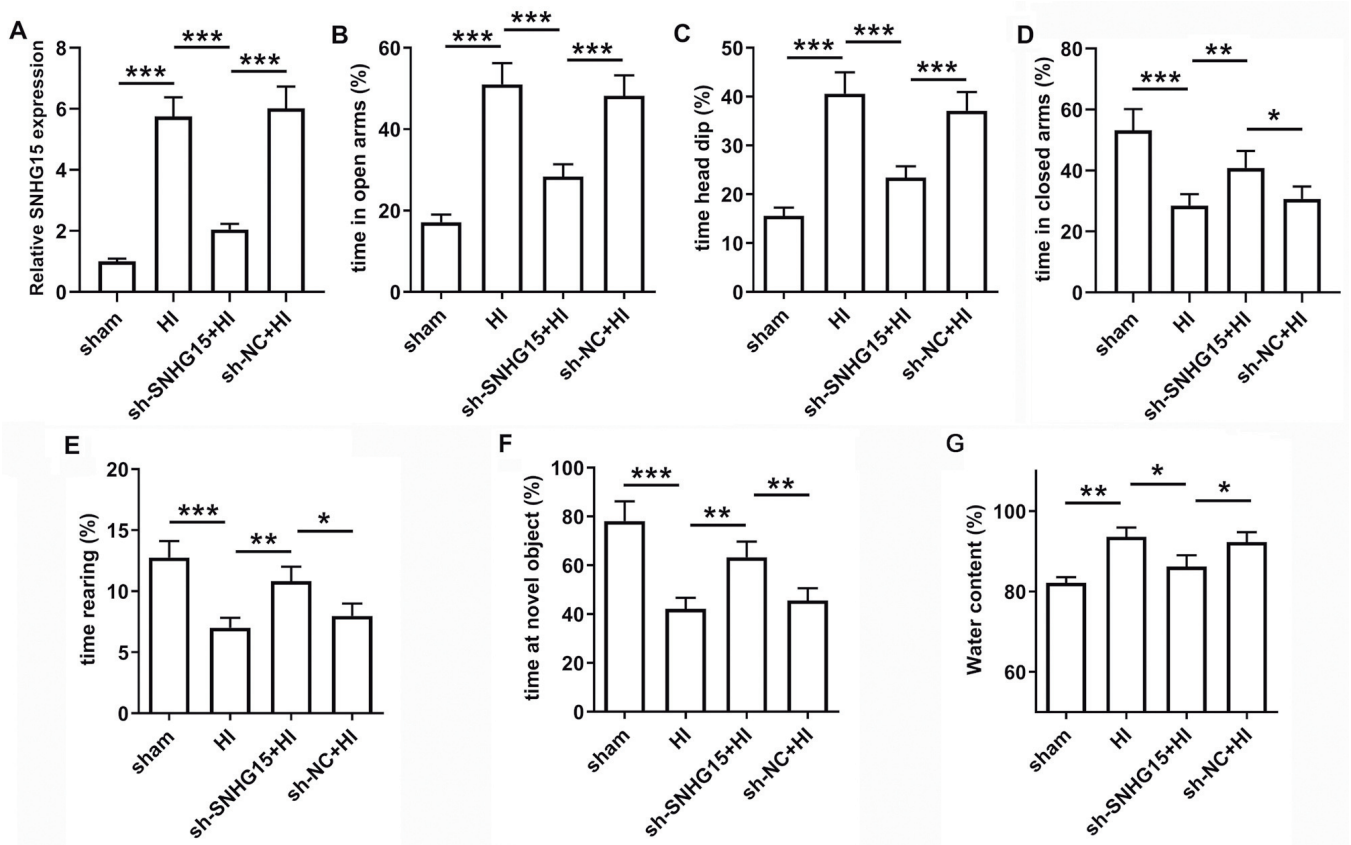

Fig. 2. Knockdown of SNHG15 attenuated HI-induced impairment of neurobehavioral function and brain edema. **A.** The expression of SNHG15 was determined using qRT-PCR in mice with HI brain injury after injection with shRNA against SNHG15. **B-E.** The neurobehavioral function of mice in HI group after injection with shRNA against SNHG15 was evaluated using elevated plus-maze. During the test, the behavioral patterns, including the time spent in open arms **(B)**, head dips time **(C)**, time spent in closed arms **(D)**, rearing time **(E)**, and time spent in novel object **(F)** were recorded. **G.** The water content of mice with HI brain injury after injection with shRNA against SNHG15 was determined. *: P<0.05; **: P<0.01; ***: P<0.001.

al., 2019). Bioinformatics analysis revealed that SNHG15 might target miR-153-3p. miR-153-3p was decreased in mice with HI brain injury, while down-regulation of SNHG15 increased the expression of miR-153-3p (P<0.001, Fig. 4A). These results further implied that SNHG15 might bind to miR-153-3p. The potential binding sites between SNHG15 and miR-153-3p and mutant sites are listed in Fig. 4B. To further demonstrate the relationship between SNHG15 and miR-153-3p, luciferase assay was performed. Results showed that miR-153-3p mimics significantly decreased wild SNHG15 reporter activity but did not affect the activity of mutant SNHG15 reporter (P<0.001, Fig. 4C). Besides, we explored the relationship of SNHG15 and miR-153-3p in OGD-induced PC12 cells. The siRNA against SNHG15 were introduced into PC12 cells and the knockout efficiency of si-SNHG15 was verified using qRT-PCR. The si-SNHG15 with the highest knockout efficiency were selected for subsequent experiments. In the OGD cell model, SNHG15 expression was increased, si-SNHG15 significantly inhibited the expression of SNHG15 (all P<0.001, Fig. 4D). Furthermore, miR-153-3p was decreased in OGD cells, which was reversed by down-regulated SNHG15 (all P<0.001, Fig. 4E). These results indicated that SNHG15 acted as a miR-153-3p sponge.

SETD7 was a target of miR-153-3p

Evidence proved that miRNAs usually played roles through targeting mRNAs. Bioinformatics analysis found that SETD7 was a potential target of miR-153-3p. The mRNA and protein levels of SETD7 was increased in mice with HI brain injury, and down-regulation of SNHG15 decreased the expression of SETD7 (P<0.01, Fig. 5A,B). The sequences of putative binding sites between miR-153-3p and SETD7 and mutant sites are shown in Fig. 5C. The binding relationship between miR-153-3p and SETD7 was better verified by luciferase assay. We found that miR-153-3p mimics significantly inhibited the activity of wild 3'-UTR of SETD7 while they had no effects on the activity of mutant 3'-UTR of SETD7 (P<0.001, Fig. 5D). Besides, overexpression of miR-153-3p decreased the mRNA and protein levels of SETD7 in OGD-induced PC12 cells, and down-regulation of miR-153-3p increased the expression of SETD7 (all P<0.001, Fig. 5E,F). Furthermore, we found that elevated SETD7 in OGD-induced PC12 cells was suppressed by decreased SNHG15 (all P<0.001, Fig. 5G,H). Thus, these findings revealed that SETD7 was a target of miR-153-3p.

SNHG15 regulated cell apoptosis induced by OGD through modulating miR-153-3p/SETD7 axis

According to the relationship among SNHG15, miR-153-3p, and SETD7 in the above results, we studied whether the miR-153-3p/SETD7 axis mediated the regulation of SNHG15 on HI brain injury. First, the siRNA against SETD7 were introduced into PC12 cells.

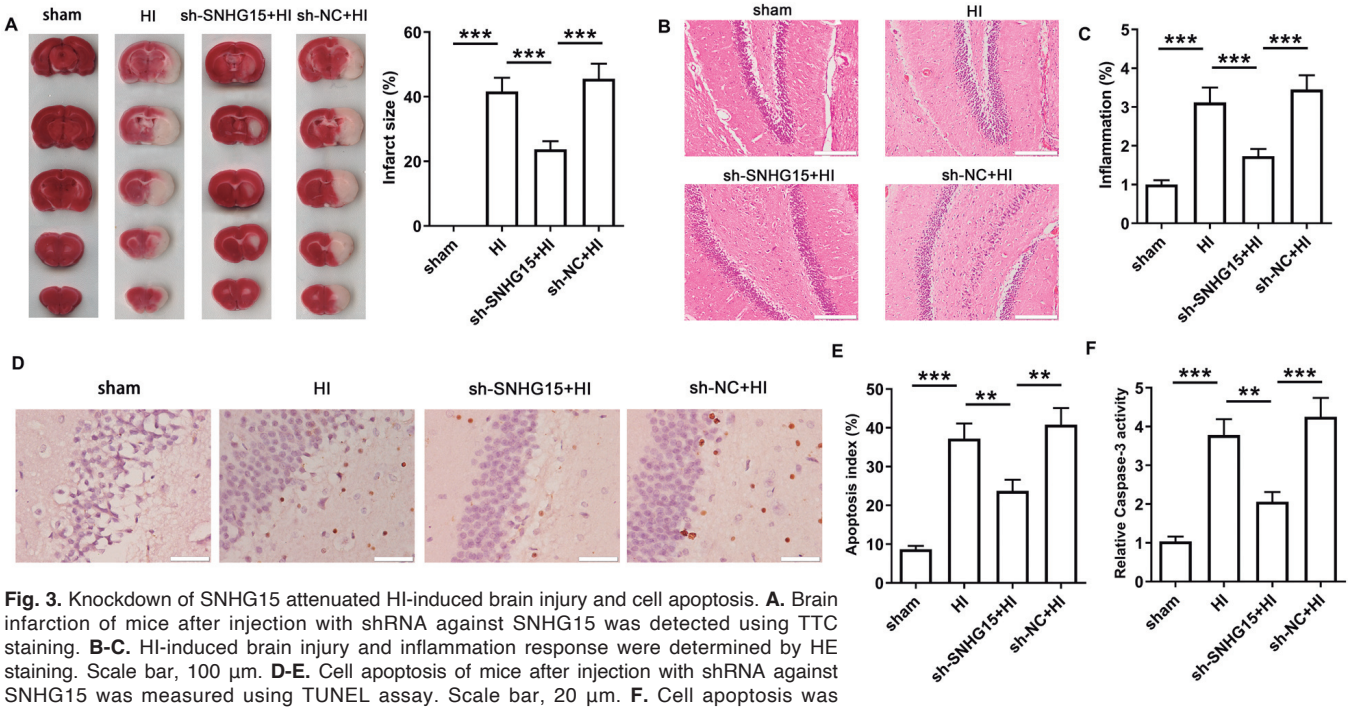

Fig. 3. Knockdown of SNHG15 attenuated HI-induced brain injury and cell apoptosis. **A.** Brain infarction of mice after injection with shRNA against SNHG15 was detected using TTC staining. **B-C.** HI-induced brain injury and inflammation response were determined by HE staining. Scale bar, 100 μm. **D-E.** Cell apoptosis of mice after injection with shRNA against SNHG15 was measured using TUNEL assay. Scale bar, 20 μm. **F.** Cell apoptosis was investigated by determining the activity of caspase-3. **: P<0.01; ***: **P**<0.001.

The knockout efficiency of si-SETD7 was verified using qRT-PCR (all $P<0.001$, Fig. 6A). The si-SETD7 with the highest knockout efficiency were selected for subsequent experiments. In P12 cells, elevated SETD7 induced by OGD was decreased by down-regulated SNHG15 and increased by down-regulated miR-153-3p. However, knockdown of SETD7 reversed the action of SNHG15 and miR-153-3p on SETD7 expression (all $P<0.01$, Fig. 6B,C). CCK-8 assay showed that the OGD-induced inhibition of cell viability was increased by down-regulated SNHG15 but decreased by down-regulated miR-153-3p, which was abrogated by decreased SETD7 (all $P<0.01$, Fig. 6D). Besides, the LDH level and caspase-3 activity were decreased by down-regulated SNHG15 but were increased by down-regulated miR-153-3p, which was further reversed by decreased SETD7 in OGD-induced PC12 cells (all $P<0.01$, Fig. 6E,F). Furthermore, flow cytometry and TUNEL assay showed that the OGD-induced cell apoptosis was inhibited by decreased SNHG15 while being increased by decreased miR-153-3p, which was further reversed by decreased SETD7 (all $P<0.05$, Fig. 6G,H and Fig. 7A,B).

Discussion

Perinatal hypoxic-ischemic encephalopathy (HIE) is a common disease in newborns accompanied by high morbidity, and it usually leads to severe brain injury (Sun et al., 2014; Lu et al., 2015). Due to lack of effective therapy strategies, most HIE survival patients

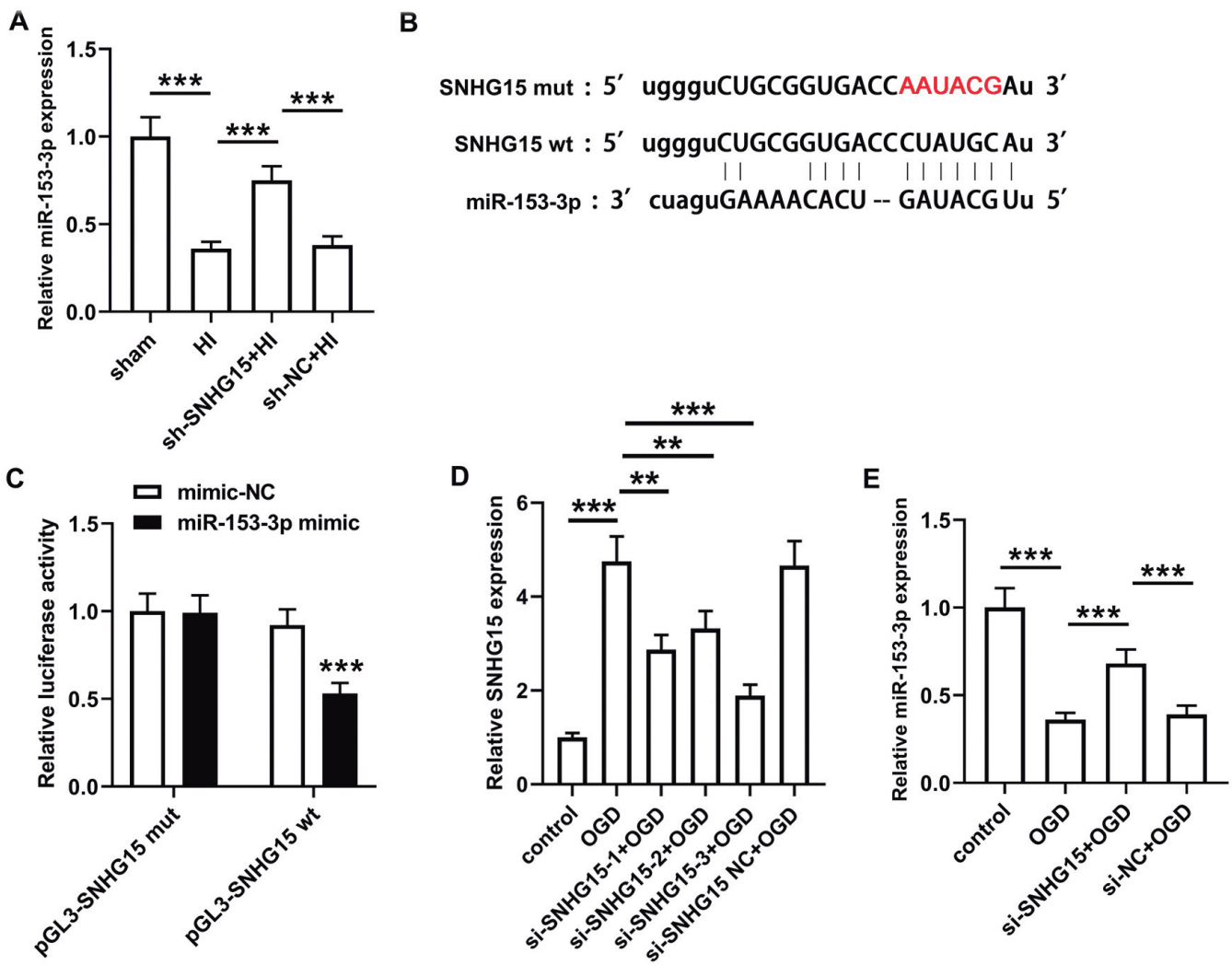

Fig. 4. SNHG15 acted as a sponge of miR-153-3p. **A.** The expression of miR-153-3p in mice with HI brain injury after injection with shRNA against SNHG15 was determined using qRT-PCR. **B.** The putative binding sites of SNHG15 and miR-153-3p and mutant sites were shown. **C.** Whether SNHG15 directly targeted miR-153-3p in PC12 cells was determined by luciferase assay. **D.** The expression of SNHG15 was detected by qRT-PCR in OGD-induced PC12 cells and transfected with si-SNHG15s. **E.** The expression of miR-153-3p in OGD-induced PC12 cell and transfected with si-SNHG15 were measured using qRT-PCR. ***: $P<0.001$.

suffer cognitive impairment and long-term neurological disabilities (Zhao et al., 2020a). Therefore, it is a significant threat to public health. Increasing studies reported that lncRNAs participated in the regulation of HI damage (Li et al., 2019; Wang and Yuan, 2019; Zhao et al., 2020a). LncRNA SNHG15 was elevated in acute ischemic stroke patients, and it alleviated cerebral ischemia-reperfusion injury (Deng et al., 2018; Wen et al., 2020). Therefore, we speculated that SNHG15 might be involved in the regulation of HI brain injury.

To study the action of SNHG15 on HI brain injury, the expression of SNHG15 in HI brain injury was explored. The findings revealed that SNHG15 was elevated in brain tissues of mice with HI brain injury, which was consistent with previous studies (Deng et al., 2018; Guo et al., 2020). Deng et al. described that the level of SNHG15 was increased in acute ischemic stroke patients (Deng et al., 2018). Guo et al. revealed that

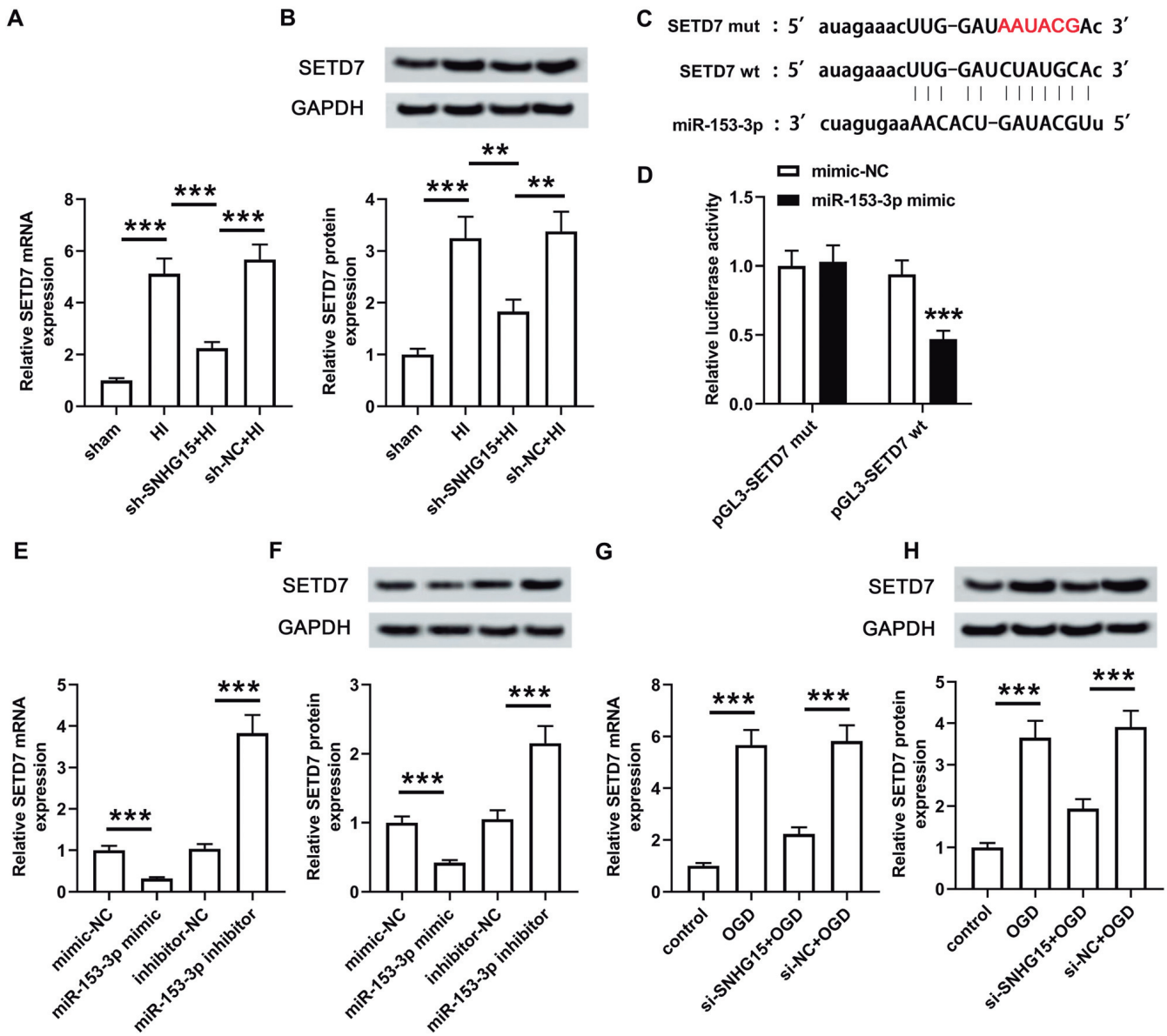

Fig. 5. SETD7 was a target of miR-153-3p. **A.** The mRNA level of SETD7 was determined by qRT-PCR in mice with HI brain injury after injection with sh-SNHG15. **B.** The protein level of SETD7 in mice with HI brain injury after injection with sh-SNHG15 was detected using Western blot. **C.** The putative binding sites of miR-153-3p and SETD7 and mutant sites were presented. **D.** Whether SETD7 was a target of miR-153-3p in PC12 cells was verified by luciferase assay. **E.** The mRNA expression of SETD7 in PC12 cells transfected with miR-153-3p mimic or inhibitor was measured by qRT-PCR. **F.** The protein level of SETD7 in PC12 cells transfected with miR-153-3p mimic or inhibitor was measured by Western blot. **G.** The mRNA expression of SETD7 in PC12 cells transfected with si-SNHG15 was detected using qRT-PCR assay. **H.** The protein level of SETD7 in PC12 cells transfected with si-SNHG15 was quantified by Western blot. **: P<0.01; ***: P<0.001.

SNHG15 was overexpressed in middle cerebral artery occlusion (MCAO)-induced mice and OGD-induced N2a cells (Guo et al., 2020). The aberrant expression of SNHG15 in brain tissues with HI injury implied that SNHG15 might play a regulation role in HI brain injury. Therefore, the effect of SNHG15 on HI brain injury was explored. Because HI brain injury is the leading cause of neurobehavioral and cognitive dysfunction (Lim et al., 2020), the effects of SNHG15 on neurobehavioral function of mice with HI brain injury was studied. The results suggested that SNHG15 attenuated HI-induced impairment of neurobehavioral function. Brain edema was considered as a prominent feature of human perinatal cerebral HI injury (Mujsce et al., 1990). Our results revealed that the brain water content after HI injury was increased, but was alleviated by SNHG15. Up to now, there has been no study reporting the regulation of SNHG15 on neurobehavioral function and edema induced by HI brain injury. In brief, these results indicated that SNHG15 attenuated HI-induced

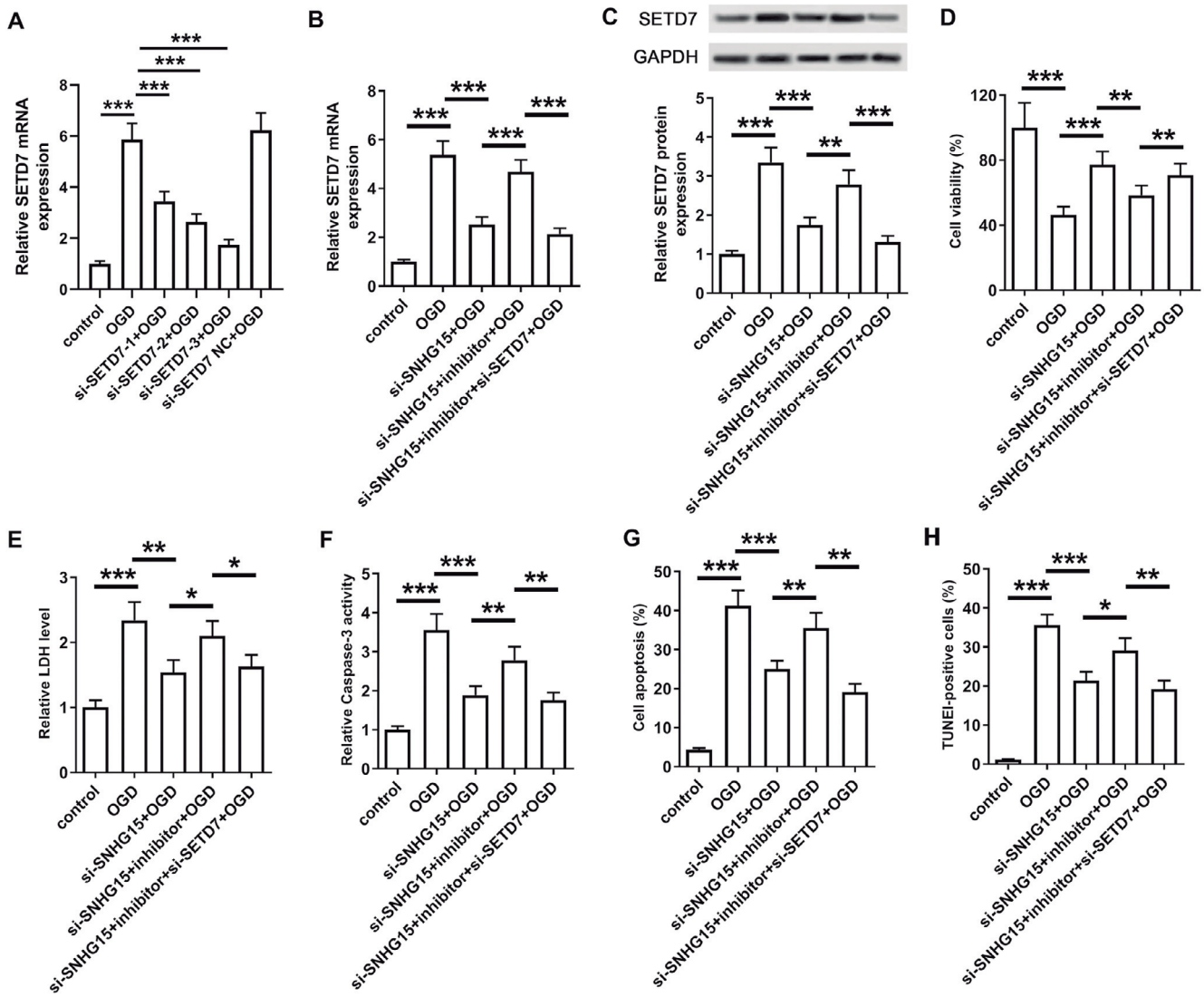

Fig. 6. SNHG15 regulated cell apoptosis induced by OGD through modulating the miR-153-3p/SETD7 axis. **A.** The expression of SETD7 in OGD-induced PC12 cells and transfected with si-SETD7s was determined by qRT-PCR. **B.** The mRNA expression of SETD7 in OGD-induced PC12 cells and transfected with si-SNHG15, miR-153-3p inhibitor, or si-SETD7 was measured by qRT-PCR. **C.** The protein level of SETD7 in OGD-induced PC12 cells and transfected with si-SNHG15, miR-153-3p inhibitor, or si-SETD7 was measured by Western blot. **D.** Cell viability of OGD-induced PC12 cells and transfected with si-SNHG15, miR-153-3p inhibitor or si-SETD7 was measured by CCK-8 assay. **E.** The LDH level in OGD-induced PC12 cells and transfected with si-SNHG15, miR-153-3p inhibitor or si-SETD7 was measured. **F.** The caspase-3 activity of OGD-induced PC12 cells and transfected with si-SNHG15, miR-153-3p inhibitor, or si-SETD7 was determined. **G.** Cell apoptosis proportion of OGD-induced PC12 cells and transfected with si-SNHG15, miR-153-3p inhibitor, or si-SETD7 was measured using Flow cytometry. **H.** Cell apoptosis of OGD-induced PC12 cells and transfected with si-SNHG15, miR-153-3p inhibitor, or si-SETD7 was measure by TUNEL assay. Scale bar, 200 μm. *: $P<0.05$; **: $P<0.01$; ***: $P<0.001$.

impairment of neurobehavioral function and brain edema.

To further investigate the effect of SNHG15 on HI brain injury, brain tissue injury, inflammation and apoptosis were explored. Our findings revealed that knockdown of SNHG15 attenuated HI injury-induced brain tissue damage, inflammation and apoptosis. These results were similar to the findings obtained in previous studies (Guo et al., 2020; Wen et al., 2020). Guo et al. reported that silenced SNHG15 attenuated brain infarction and the levels of pro-inflammatory cytokines in brain tissues of MCAO-induced mice, and suppressed OGD-induced N2a cell apoptosis (Guo et al., 2020). Wen et al. discovered that cell apoptosis induced by cerebral ischemia-reperfusion (I/R) and oxygen-glucose deprivation/reoxygenation (OGD/R) was inhibited by decreased SNHG15 (Wen et al., 2020). Taken together, knockdown of SNHG15 attenuated HI-induced brain injury and cell apoptosis.

LncRNAs usually modulate gene expression via serving as miRNAs sponges, thereby regulating disease progression (Chan and Tay, 2018). For example,

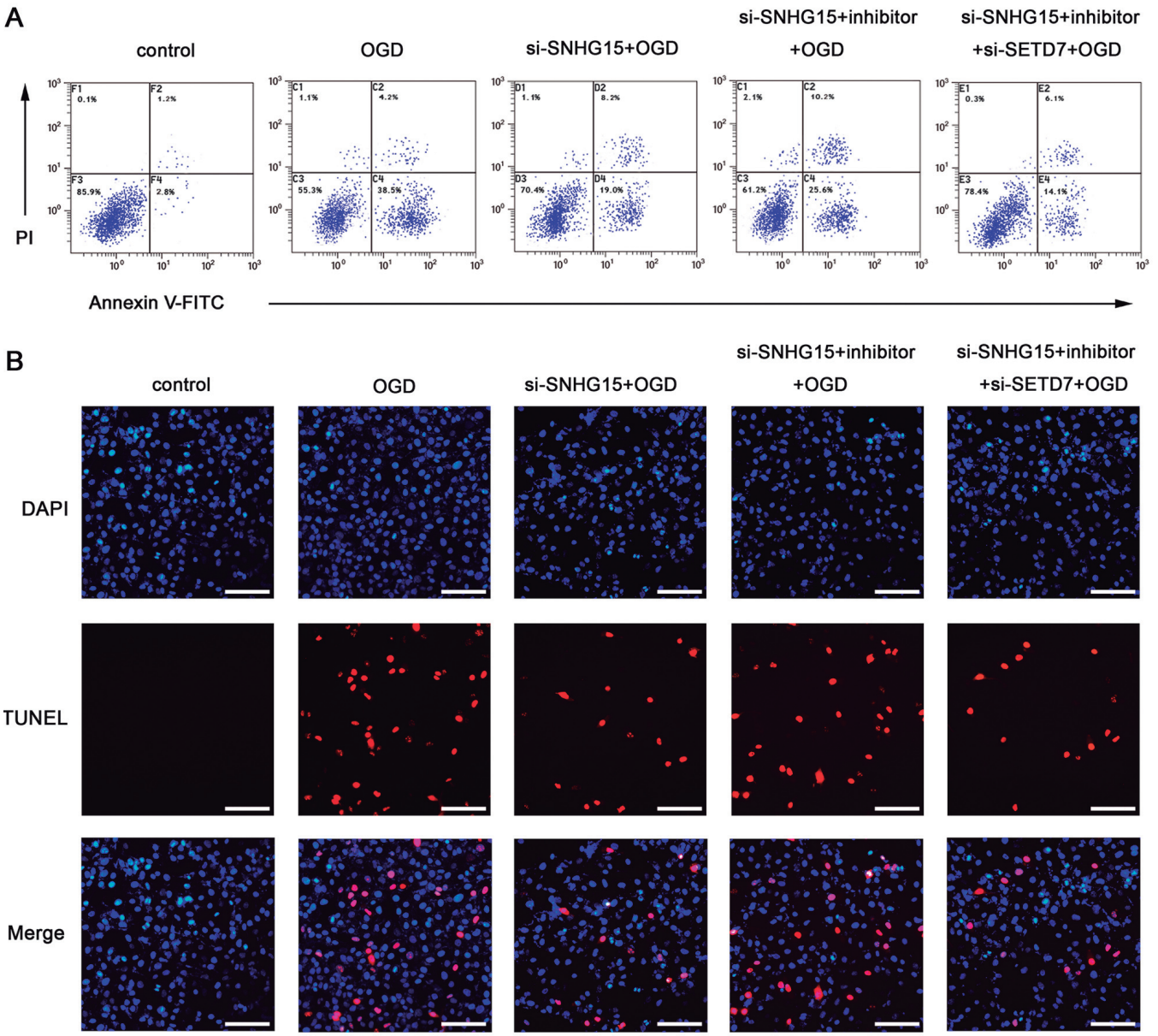

Fig. 7. Cell apoptosis detection of PC12 cells. **A.** Representative images of Flow cytometry in OGD-induced PC12 cells and transfected with si-SNHG15, miR-153-3p inhibitor, or si-SETD7. **B.** Representative images of TUNEL assay in OGD-induced PC12 cells and transfected with si-SNHG15, miR-153-3p inhibitor, or si-SETD7.

lncRNA GAS5 regulated ischemic stroke by acting as a miR-137 sponge to modulate the Notch1 signaling pathway (Chen et al., 2018). Besides, SNHG15 modulated YAP1-Hippo signaling pathway in papillary thyroid carcinoma via sponging miR-200a-3p (Wu et al., 2018). Furthermore, SNHG15 protected against cerebral I/R injury by modulating FOXO1 expression via sponging miR-183-5p (Wen et al., 2020). Therefore, we inferred that SNHG15 might exert a regulatory role in HI brain injury via ceRNA mechanism. Thus, to elucidate the underlying mechanism of SNHG15 on HI brain injury, the potential miRNA targets of SNHG15 were explored. Results showed that SNHG15 acted as a miR-153-3p sponge. miR-153-3p was decreased in OGD-induced PC12 cells, and miR-153-3p expression was negatively regulated by SNHG15. The results were in accordance with the results concluded by Wang et al. (Wang et al., 2020). They found that miR-153-3p was significantly decreased in neurons with I/R injury *in vivo* and OGD/R injury *in vitro* (Wang et al., 2020). In a word, these results indicated that SNHG15 acted as a miR-153-3p sponge.

MiRNAs usually play roles in diseases via inhibiting the target gene expression through targeting to 3'-UTR of the gene (Chan and Tay, 2018). For example, upregulated miR-29b promoted neuronal cell death through inhibiting the expression of target gene Bcl2L2 after ischemic brain injury (Shi et al., 2012). MiR-191 inhibited angiogenesis after acute ischemic stroke through modulating VEZF1 expression (Du et al., 2019). Therefore, the target gene of miR-153-3p was screened in this study. Results revealed that SETD7 was a target of miR-153-3p. SETD7 was increased in OGD-induced PC12 cells, and the expression of SETD7 was negatively regulated by miR-153-3p and positively modulated by SNHG15. A previous study proved that SETD7 was increased in cardiomyocytes in response to hypoxia/reoxygenation (H/R) injury (Dang et al., 2018). Besides, SETD7 was also elevated in myocardial tissues after ischemic injury (Ambrosini et al., 2020). In brief, these findings revealed that SETD7 was a target of miR-153-3p.

According to the relationship among SNHG15, miR-153-3p, and SETD7 in the above results, we inferred that SETD7 might mediate the regulation of SNHG15 on HI brain injury through sponging miR-153-3p. Therefore, to explore the underlying mechanism of SNHG15 on HI brain injury, the roles of miR-153-3p and SETD7 during the regulation process were investigated. Results revealed that SNHG15 regulated OGD-induced cell apoptosis through modulating miR-153-3p/SETD7 axis. In other words, miR-153-3p and SETD7 participated in the regulation of HI brain injury. Wang et al. demonstrated that overexpression of miR-153-3p attenuated OGD/R-induced neuronal injury (Wang et al., 2020). Ning et al. found that inhibition of exosomal miR-153-3p derived from bone marrow mesenchymal stem cells ameliorated hypoxia-induced myocardial injury (Ning et al., 2021). Furthermore, the previous study proved that inhibition of SETD7 could inhibit glucose deprivation-induced mitochondrial oxidative stress and apoptosis. Besides, knockdown of SETD7 mediated the protective effects on H/R-induced cardiomyocyte injury through regulating Keap1/Nrf2 signaling (Dang et al., 2018). Taken together, SNHG15 regulated cell apoptosis induced by OGD through modulating SETD7 via sponging miR-153-3p.

This study was characterized by limitations. Conclusions in this study were obtained from preclinical animal and cell experiments, which could not be transferred to human samples. Besides, previous studies proved that induction of autophagy was critical for HI brain injury (Koike et al., 2008; Xu et al., 2016). However, the role of SNHG15 in regulation autophagy in HI brain injury was not investigated in this study, which will be studied in the future.

In conclusion, our findings provided evidence that lncRNA SNHG15 increased the expression of SETD7 to attenuate cell apoptosis and HI brain injury via sponging miR-153-3p. These findings may be profitable to HIE therapy and SNHG15 may be a prospective target for HIE therapy that deserves further investigation.

Acknowledgements. None.

Conflict of interest. The authors declare that there is no conflict of interest.

References

Abdollahzadeh R., Daraei A., Mansoori Y., Sepahvand M., Amoli M.M. and Tavakkoly-Bazzaz J. (2019). Competing endogenous RNA (ceRNA) cross talk and language in ceRNA regulatory networks: A new look at hallmarks of breast cancer. J. Cell. Physiol. 234, 10080-10100.

Ambrosini S., Montecucco F., Akhmedov A., Mohammed S., Brown P., Rossi F., Kiss A., Luscher T., Costantino S. and Paneni F. (2020). Methylation of the hippo signalling effector YAP by SETD7 drives myocardial ischemic injury. Eur. Heart J. 41, ehaa946.3636.

Bai J., Xu J., Zhao J. and Zhang R. (2020). LncRNA NBR2 suppresses migration and invasion of colorectal cancer cells by downregulating miRNA-21. Hum. Cell 33, 98-103.

Cao Y., Liu H., Zhang J. and Dong Y. (2020). Circular RNA cZNF292 silence alleviates OGD/R-induced injury through up-regulation of miR-22 in rat neural stem cells (NSCs). Artif. Cells Nanomed. Biotechnol. 48, 594-601.

Chan J.J. and Tay Y. (2018). Noncoding RNA:RNA regulatory networks in Cancer. Int. J. Mol. Sci. 19, 1310.

Chen F., Zhang L., Wang E., Zhang C. and Li X. (2018). LncRNA GAS5 regulates ischemic stroke as a competing endogenous RNA for miR-137 to regulate the Notch1 signaling pathway. Biochem. Biophys. Res. Commun. 496, 184-190.

Chen H., Hu X., Li R., Liu B., Zheng X., Fang Z., Chen L., Chen W., Min L. and Hu S. (2020). LncRNA THRIL aggravates sepsis-induced acute lung injury by regulating miR-424/ROCK2 axis. Mol. Immunol. 126, 111-119.

Cong Z., Diao Y., Xu Y., Li X., Jiang Z., Shao C., Ji S., Shen Y., De W. and Qiang Y. (2019). Long non-coding RNA linc00665 promotes

lung adenocarcinoma progression and functions as ceRNA to regulate AKR1B10-ERK signaling by sponging miR-98. Cell Death Dis. 10, 1-15.

Dang Y., Ma X., Li Y., Hao Q., Xie Y., Zhang Q., Zhang F. and Qi X. (2018). Inhibition of SETD7 protects cardiomyocytes against hypoxia/reoxygenation-induced injury through regulating Keap1/Nrf2 signaling. Biomed. Pharmacother. 106, 842-849.

Deng Q.-W., Li S., Wang H., Sun H.-L., Zuo L., Gu Z.-T., Lu G., Sun C.-Z., Zhang H.-Q. and Yan F.-L. (2018). Differential long noncoding RNA expressions in peripheral blood mononuclear cells for detection of acute ischemic stroke. Clin. Sci. 132, 1597-1614.

Du K., Zhao C., Wang L., Wang Y., Zhang K.Z., Shen X.Y., Sun H.X., Gao W. and Lu X. (2019). MiR-191 inhibit angiogenesis after acute ischemic stroke targeting VEZF1. Aging (Albany NY). 11, 2762-2786.

Fang H., Li H.F., He M.H., Yan J.Y., Yang M., Zhang F.X., Wang R.R., Wang Q.Y. and Zhang J.P. (2019). Long non-coding RNA MALAT1 sponges microRNA-429 to regulate apoptosis of hippocampal neurons in hypoxic-ischemic brain damage by regulating WNT1. Brain. Res. Bull. 152, 1-10.

Geisler S. and Coller J. (2013). RNA in unexpected places: long non-coding RNA functions in diverse cellular contexts. Nat. Rev. Mol. Cell. Biol. 14, 699-712.

Guo T., Liu Y., Ren X., Wang W. and Liu H. (2020). Promoting role of long non-coding RNA small nucleolar RNA host gene 15 (SNHG15) in neuronal injury following ischemic stroke via the microRNA-18a/CXC chemokine ligand 13 (CXCL13)/ERK/MEK axis. Med. Sci. Monit. 26, e923610-1.

Huang L., Lin H., Kang L., Huang P., Huang J., Cai J., Xian Z., Zhu P., Huang M. and Wang L. (2019). Aberrant expression of long noncoding RNA SNHG15 correlates with liver metastasis and poor survival in colorectal cancer. J. Cell. Physiol. 234, 7032-7039.

Koike M., Shibata M., Tadakoshi M., Gotoh K., Komatsu M., Waguri S., Kawahara N., Kuida K., Nagata S. and Kominami E. (2008). Inhibition of autophagy prevents hippocampal pyramidal neuron death after hypoxic-ischemic injury. Am. J. Pathol. 172, 454-469.

Kong Q. and Qiu M. (2018). Long noncoding RNA SNHG15 promotes human breast cancer proliferation, migration and invasion by sponging miR-211-3p. Biochem. Biophys. Res. Commun. 495, 1594-1600.

Kong X., Duan Y., Sang Y. and Li Y. (2019). LncRNA-CDC6 promotes breast cancer progression and function as ceRNA to target CDC6 by sponging microRNA-215. J. Cell. Physiol. 234, 9105-9117.

Li D., Wang J., Zhang M., Hu X., She J., Qiu X., Zhang X., Xu L., Liu Y. and Qin S. (2020). LncRNA MAGI2-AS3 is regulated by BRD4 and promotes gastric cancer progression viamaintaining ZEB1 overexpression by sponging miR-141/200a. Mol. Ther. Nucleic. Acids 19, 109-123.

Li E.-y., Zhao P.-j., Jian J., Yin B.-q., Sun Z.-y., Xu C.-x., Tang Y.-c. and Wu H. (2019). LncRNA MIAT overexpression reduced neuron apoptosis in a neonatal rat model of hypoxic-ischemic injury through miR-211/GDNF. Cell Cycle 18, 156-166.

Lim K.H., Yang S., Kim S.H. and Chun S. (2020). Discoveries for long non-coding RNA dynamics in traumatic brain injury. Biology (Basel). 9, 458.

Lu Q., Harris V.A., Kumar S., Mansour H.M. and Black S.M. (2015). Autophagy in neonatal hypoxia ischemic brain is associated with oxidative stress. Redox. Biol. 6, 516-523.

Ma Q., Dasgupta C., Li Y., Huang L. and Zhang L. (2017). MicroRNA-210 suppresses junction proteins and disrupts blood-brain barrier integrity in neonatal rat hypoxic-ischemic brain injury. Int. J. Mol. Sci. 18, 1356.

Mi H., Wang X., Wang F., Li L., Zhu M., Wang N., Xiong Y. and Gu Y. (2020). SNHG15 contributes to cisplatin resistance in breast cancer through sponging miR-381. Onco. Targets. Ther. 13, 657-666.

Mujsce D.J., Towfighi J., Stern D. and Vannucci R.C. (1990). Mannitol therapy in perinatal hypoxic-ischemic brain damage in rats. Stroke 21, 1210-1214.

Ning W., Li S., Yang W., Yang B., Xin C., Ping X., Huang C., Gu Y. and Guo L. (2021). Blocking exosomal miRNA-153-3p derived from bone marrow mesenchymal stem cells ameliorates hypoxia-induced myocardial and microvascular damage by targeting the ANGPT1-mediated VEGF/PI3k/Akt/eNOS pathway. Cell. Signal. 77, 109812.

Rice J.E. 3rd, Vannucci R.C. and Brierley J.B. (1981). The influence of immaturity on hypoxic-ischemic brain damage in the rat. Ann. Neurol. 9, 131-141.

Rostami E., Davidsson J., Ng K.C., Lu J., Gyorgy A., Walker J., Wingo D., Plantman S., Bellander B.M., Agoston D.V. and Risling M. (2012). A model for mild traumatic brain injury that induces limited transient memory impairment and increased levels of axon related serum biomarkers. Front. Neurol. 3, 115.

Shen Y., Liu S., Fan J. and Jin Y. (2017). Nuclear retention of the lncRNA SNHG1 by doxorubicin attenuates hnRNPC-p53 protein interactions. EMBO Rep. 18, 536-548.

Shi G., Liu Y., Liu T., Yan W., Liu X., Wang Y., Shi J. and Jia L. (2012). Upregulated miR-29b promotes neuronal cell death by inhibiting Bcl2L2 after ischemic brain injury. Exp. Brain Res. 216, 225-230.

Sun J., Qu Y., He H., Fan X., Qin Y., Mao W. and Xu L. (2014). Protective effect of polydatin on learning and memory impairments in neonatal rats with hypoxic-ischemic brain injury by up-regulating brain-derived neurotrophic factor. Mol. Med. Rep. 10, 3047-3051.

Sun D., Mu Y. and Piao H. (2018). MicroRNA-153-3p enhances cell radiosensitivity by targeting BCL2 in human glioma. Biol. Res. 51, 1-10.

Tong R., Zhang J., Wang C., Li X., Yu T. and Wang L. (2020). LncRNA PTCSC3 inhibits the proliferation, invasion and migration of cervical cancer cells via sponging miR-574-5p. Clin. Exp. Pharmacol. Physiol. 47, 439-448.

Tu L., Wang Y., Chen D., Xiang P., Shen J., Li Y. and Wang S. (2018). Protective effects of notoginsenoside R1 via regulation of the PI3K-Akt-mTOR/JNK pathway in neonatal cerebral hypoxic-ischemic brain injury. Neurochem. Res. 43, 1210-1226.

Wang H.-J., Tang X.L., Huang G., Li Y.B., Pan R.H., Zhan J., Wu Y.K., Liang J.F., Bai X.X. and Cai J. (2020). Long non-coding KCNQ1OT1 promotes oxygen-glucose-deprivation/reoxygenation-induced neurons injury through regulating mIR-153-3p/FOXO3 axis. J. Stroke Cerebrovasc. Dis. 29, 105126.

Wen Y., Zhang X., Liu X., Huo Y., Gao Y. and Yang Y. (2020). Suppression of lncRNA SNHG15 protects against cerebral ischemia-reperfusion injury by targeting miR-183-5p/FOXO1 axis. Am. J. Transl. Res. 12, 6250.

Wu D.M., Wang S., Wen X., Han X.R., Wang Y.J., Shen M., Fan S.H., Zhang Z.F., Shan Q., Li M.Q., Hu B., Lu J., Chen G.Q. and Zheng Y.L. (2018). LncRNA SNHG15 acts as a ceRNA to regulate YAP1-Hippo signaling pathway by sponging miR-200a-3p in papillary thyroid carcinoma. Cell. Death. Dis. 9, 947.

Xu Y., Tian Y., Tian Y., Li X. and Zhao P. (2016). Autophagy activation involved in hypoxic-ischemic brain injury induces cognitive and memory impairment in neonatal rats. J. Neurochem. 139, 795-805.

Xue H., Xu Y., Wang S., Wu Z.Y., Li X.Y., Zhang Y.H., Niu J.Y., Gao Q.S. and Zhao P. (2019). Sevoflurane post-conditioning alleviates neonatal rat hypoxic-ischemic cerebral injury via Ezh2-regulated autophagy. Drug Des. Devel. Ther. 13, 1691-1706.

Yang Q., Wu M.F., Zhu L.H., Qiao L.X., Zhao R.B. and Xia Z.K. (2020). Long non-coding RNA Snhg3 protects against hypoxia/ischemia-induced neonatal brain injury. Exp. Mol. Pathol. 112, 104343.

Ye J., Tan L., Fu Y., Xu H., Wen L., Deng Y. and Liu K. (2019). LncRNA SNHG15 promotes hepatocellular carcinoma progression by sponging miR-141-3p. J. Cell. Biochem. 120, 19775-19783.

Zhang W., Zhang H., Mu H., Zhu W., Jiang X., Hu X., Shi Y., Leak R.K., Dong Q., Chen J. and Gao Y. (2016). Omega-3 polyunsaturated fatty acids mitigate blood-brain barrier disruption after hypoxic-ischemic brain injury. Neurobiol. Dis. 91, 37-46.

Zhao J., He L. and Yin L. (2020a). lncRNA NEAT1 Binds to miR-339-5p to increase HOXA1 and alleviate ischemic brain damage in neonatal mice. Mol. Ther. Nucleic Acids 20, 117-127.

Zhao M., Wang K., Shang J., Liang Z., Zheng W. and Gu J. (2020b). MiR-345-5p inhibits tumorigenesis of papillary thyroid carcinoma by targeting SETD7. Arch. Med. Sci. 16, 888.

Zhu J.R., Tao Y.F., Lou S. and Wu Z.M. (2010). Protective effects of ginsenoside Rb(3) on oxygen and glucose deprivation-induced ischemic injury in PC12 cells. Acta Pharmacol. Sin. 31, 273-280.

Accepted July 5, 2022